

Tomography using multiple wavelengths in digital holography: Method, simulations and experiments

Frédéric Montfort^a, Florian Charrière^b, Tristan Colomb^b, Jonas Kuehn^b, Etienne Cuche^a and Christian Depeursinge^b

^aLyncée Tec, PSE - A, CH-1015 Lausanne, Switzerland;

^bEcole Polytechnique Fédérale de Lausanne (EPFL), Institut d'Optique Appliquée, CH-1015 Lausanne, Switzerland

ABSTRACT

In this paper we present a method for tomographic imaging using multiple wavelengths in digital holographic microscopy. This method is based on the recording at different wavelengths equally separated in the k -domain, in off-axis geometry, of the interference between a reference wave and an object wave reflected by a microscopic sample and magnified by a microscope objective. A couple charged device (CCD) camera records consecutively the resulting holograms, which are then numerically reconstructed to obtain their resulting wavefront. Those wavefronts are then summed. The result of this operation is a constructive addition of complex waves in the selected plane and destructive addition in the others. Varying the plane of interest enables the scan the object in depth.

For the presented simulations and experiments, twenty wavelengths are used in the 480-700 nm range. An object consisting of irregularly stairs with heights of 375, 525, 975, 1200 and 1275 nm is reconstructed. Its lateral dimensions are 250×250 microns. The results show clearly a 3D imaging technique with axial resolution under the micron.

Keywords: Digital holography, Image reconstruction technique, Microscopy, Tomography, Three-dimensional image acquisition

1. INTRODUCTION

The principles of holography have been known for a long time and have been recognized as being an attractive technique for practical applications in various domains, such as optical metrology.^{1,2} Nowadays, a renewal of holographic techniques can be observed thanks to the use of electronic camera and digital data processing techniques. Since 1994, some authors have proposed the use of a coupled charged device (CCD) camera and an ordinary computer to reconstruct directly the wavefront from a hologram.³ This approach is generally called "Digital Holography" and has been proved efficient, especially in metrology. New perspective have been opened by the introduction of a precise method to evaluate simultaneously quantitative phase and amplitude contrast by the digital processing of a single hologram taken in an off axis geometry.⁴ Pioneering work in Digital Holographic Microscopy (DHM) has been done by applying this method to microscopy.⁵ This made possible the derivation of precise and quantitative data (intensity and phase) on the wavefront outgoing from a reflective and/or (semi-) transparent object. In some cases, the surface and volume of homogeneous objects like single cells with well resolved forms, can be reconstructed in 3-D and with nanometric resolution along the optical axis.^{6,7} Moreover, using this technique, 3-D objects can be reconstructed much faster than in more classical or scanning methods.

Digital holographic microscopy uses of a single hologram taken at a single wavelength and with a single propagation direction of the illuminating wave (single k -vector). Thus, the image also contains information coming from the upper and lower sections of the object which blur the image and makes this method more suitable for thin objects. Nevertheless, an approach to solve this problem in a reflection configuration consists in reducing the coherence length of the source in order to attenuate the contribution of the "out of focus" sections

Further author information: (Send correspondence to Christian Depeursinge)

Christian Depeursinge: E-mail: christian.depeursinge@epfl.ch, Telephone: +41 21 693 61 77

Frédéric Montfort: E-mail: frederic.montfort@lynceetec.com, Telephone: +41 21 693 02 27

of the object.^{8,9} In this case the thickness of the remaining section is given by the coherence length of the light source, typically several tenths of microns.

Furthermore, the topology of the object is given by the phase information and so it suffers from the phase wrapping problems which means that the object has to induce a phase shift smaller than the wavelength. It is often not the case and thus an algorithm is needed to unwrap the collected phase. Although these techniques are efficient for relatively smooth objects, their results are in most cases wrong when abrupt edges higher than the wavelength are encountered making the use of DHM with relatively thick objects difficult.

The proposed method uses variable wavelengths illumination waves. The reciprocal space is then scanned by changing the diameter of the Ewald sphere. The 3-D image can be computed by the 3-D Fourier transform of the reciprocal space. This technique, developed along the guidelines fixed by the diffraction tomography theorem (see also the pioneering works¹⁰⁻¹³), may appear as rather complex and cumbersome in its practical application. Digital holography yields a particularly simple way to express "indirectly" the diffraction tomography theorem: remaining in the direct space, tomography of the object can be achieved by the superposition of reconstructed wavefronts from holograms taken at multiple wavelengths. A similar approach has already been proposed several years ago by Marron,¹⁴ who has called this method "holographic laser radar". Reference to a similar approach has also been described by Arons and Al. as "Fourier synthesis holography".¹⁵ More recently, the feasibility of section imaging by wavelength scanning digital holography has been also demonstrated by Kim^{16,17} at a macro-scale.

Nevertheless, none of these techniques works at the micro-scale. The introduction of a microscope objective in the set-up, the use of the retrieved phase for high axial precision measures and a wide wavelength range opens the field of tomography to the sub-microscopic world. Among possible applications are material and life science. Objects like micro-fluidic devices, micro mechanical systems (MEMS) and micro opto electro mechanical systems (MOEMS), semi-conductor devices can be tomographed. In life science, biological cells and tissues or their constituents (nucleus and various organelles) can be sectioned in a non-invasive way.

The aim of this work is to provide an efficient tomographic technique based on digital holographic microscopy to reconstruct, plane by plane, the 3-D object of interest without using a mechanical scanning. The reconstruction has to be fast to get images in a very short period of time with a lateral resolution up to the diffraction limit and an axial resolution under de micron

The developed method uses multi-wavelength scanning to eliminate this blurred images from "out of focus" parts of the object. Several holograms of the object are taken at different wavelengths and each corresponding electric field distribution will be reconstructed. Then, the addition of those complex electric field distributions will produce a constructive combination only in the focused plane, and a destructive one elsewhere.

2. PROPOSED METHOD

2.1. Digital Holography

Holography is a method to record and retrieve a complex wavefront. To do so, the concerned wavefront interferes with a reference wavefront to create a hologram, which intensity is recorded on a sensitive substrate. By illuminating the hologram with the same reference front, a replica of the wavefront of interest is diffracted.

In digital holography, the interference intensity is recorded on a CCD camera. The reconstruction of the hologram is done in three steps. The first one is to digitally illuminate the hologram with a wave, called reconstruction wave, having the same features as the reference wave. Then the undesired diffracted images (zero order and conjugate image) are filtered in the frequency domain.¹⁸ The last step is to propagate the reconstructed object wave from the hologram plane to its focalization plane.^{4,5} This propagation is done in the Fresnel approximation, using the convolution formulation to be sure to have an image size and position in space independent of the wavelength.¹⁹

2.2. Multiple wavelengths for tomography

To introduce the multi-wavelength approach, let us state that the diffracted fields of a single hologram Ψ_j , reconstructed in the object plane, creates an exact replica of the object wave Ψ_0 at the object. Let us also consider an object point P located at (x_0, y_0, z_0) which emits a Huyghens spherical wavelet proportional to $A(P) \exp(ikr_{PQ})$ measured at an arbitrary point $Q = (x, y, z)$, where $r_{PQ} = n|\mathbf{r}_P - \mathbf{r}_Q|$ is the optical pathlength

between P and Q , and n is the refractive index (Fig. 1). We neglect the $1/r$ dependence of the amplitude. The wave propagates along the z -direction. The factor $A(P)$ represents the field amplitude and phase at the object point. For an extended object, the field at Q is proportional to the above wavelet field integrated over all the points of the object:

$$\Psi_j(Q) \propto \iiint A(P) \exp(ikr_{PQ}) d^3\mathbf{r}_{PQ}.$$

The factor $\exp(ikr_{PQ})$ represents the propagation and diffraction of the object wave. Now assuming that a number N of copies of the electric field distribution are generated by varying the wavelength (and thus the wave number k), all the other conditions of object and illumination remaining the same, let's take N k -vectors k_j regularly separated by dk between k_{\min} and k_{\max} . We have:

$$k_{\min} = \frac{2\pi}{\lambda_{\max}}, \quad k_{\max} = \frac{2\pi}{\lambda_{\min}}, \quad dk = \frac{k_{\max} - k_{\min}}{N - 1}.$$

The result of the superposition of these electric fields at Q is:

$$\begin{aligned} \Psi(Q) &= \sum_{j=0}^{N-1} \Psi_j(Q) \\ &\propto \sum_{j=0}^{N-1} \iiint A(P) \exp(ik_j r_{PQ}) d^3\mathbf{r}_{PQ} \\ &\propto \iiint A(P) \exp(i\bar{k}r_{PQ}) \frac{\sin(dkr_{PQ} \frac{N}{2})}{\sin(dkr_{PQ} \frac{1}{2})} d^3\mathbf{r}_{PQ} \\ &\propto \iiint A(P) \exp(i\bar{k}r_{PQ}) T(r_{PQ}) d^3\mathbf{r}_{PQ}, \end{aligned}$$

where $\bar{k} = \frac{k_{\min} + k_{\max}}{2}$.

$T(r_{PQ})$ can be seen as an amplitude filter function with these extremas:

$$T(r_{PQ}) = \frac{\sin(dkr_{PQ} \frac{N}{2})}{\sin(dkr_{PQ} \frac{1}{2})} \text{ has } \begin{cases} \text{maximas for} & r_{PQ} = n \frac{2\pi}{Ndk} & n = mN \\ \text{minimas for} & r_{PQ} = n \frac{2\pi}{Ndk} & n \neq mN \end{cases}. \quad (1)$$

If we consider an infinite wavelength range, then $T(r_{PQ})$ becomes a Dirac function and the resulting wavefront $\Psi(Q)$ is non-zero only at P .

$$\lim_{N \rightarrow \infty} \Psi(Q) \propto \iiint A(P) \exp(i\bar{k}r_{PQ}) \delta(\mathbf{r}_{PQ}) d^3\mathbf{r}_{PQ} \propto A(P). \quad (2)$$

That is, for a large enough number of wave numbers k , the resultant field is proportional to the field at the object, and non-zero only at object points. In practice, if one uses a finite number N of wavelengths at regular intervals dk then the object image $A(P)$ repeats itself at axial distances $\Lambda = 2\pi/dk$ with axial resolution of $\delta = \Lambda/N$. By using appropriate values of dk and N , Λ can be matched to the axial extent of the object and δ to the desired level of axial resolution.

In a practical way, several equally k -spaced hologram are simulated or experimentally recorded and each hologram is reconstructed independently at its wavelength in amplitude and phase contrast and summed. By adjusting the phase constants of each wavefront, different planes can be sectionned. Varying the plane enables the sample to be scanned in depth.

3. SIMULATIONS & EXPERIMENTS

Simulations and experiments have been done to demonstrate the tomographic and 3D imaging abilities. To do so, twenty holograms have been simulated and experimentally recorded with regularly k-spaced wavelengths in the 480 - 700 nm range. The absolute value of the amplitude filter created by summing the given twenty wavefronts has the shape of Fig. 2. The contributions for one point in the image come from the plane of interest, but also from the points behind and in front of this plane, proportionally to this filter function. Thus, the resolution δ is given by the first zeros of the function, and the axial extent Λ by distance between two maximums. With the used parameters in a reflection set-up, the axial resolution is 725 nm and the axial extend 14.5 μm .

The used target consists of 5 reflecting steps having 375, 525, 975, 1200 and 1275 nm heights (Fig. 3). It is built by structuring silicon oxide (SiO_2) layers on a silicon wafer and recovered with 10 nm chrome and 100 nm gold for a total reflection. The sample is 250 microns large. Nevertheless, due to etching properties, the highest steps are no more rectangular, but have been attacked in the corners.

This sample has also been simulated. It is a 512×512 pixel images with 5 steps of 50×250 pixels. A wavefront reflected by this sample is simulated and propagated to the hologram plane. It is summed to a reference beam and its intensity forms the simulated hologram that is then standardly reconstructed.

The experimental set-up is based on a classical Mach-Zender off-axis holographic interferometer (Fig. 4). The light source is generated by an argon ion plasma laser (Coherent Innova 200) pumping a modelocked Ti:S laser system (Coherent Mira 900). The beam is then amplified by a regenerative amplifier (Coherent RegA 9000) and finally extended in wavelength with a tunable optical parametric amplifier (Coherent OPA 9400). The beam coming from the optical parametric amplifier (OPA) is split. On one side, the object beam illuminates the sample through the microscope objective (MO, focal length 18.4 mm, NA=0.15, magnification $\sim 10\times$) and its diffracted field, collected by the MO, interferes on the CCD with the reference beam. In our case, the interference is done in an off-axis geometry, meaning that a small angle is introduced between both waves. Two more lenses are used: one is the object beam condenser (OC) that focuses the object beam at the back focal length of the microscope objective in order to have a collimated beam illuminating the sample, and the second is the reference lens (RL) that curves the reference beam to match the curvature introduced by the microscope objective on the object beam in the CCD plane. It is to note that the image of the sample trough the MO is not focused on the CCD camera.

Two tomographic sections have been built at the heights of 0 and 525 nm. The resolution of the method is theoretically 725 nm. This gap corresponds to a total cancellation of the amplitude filter function. The nearest gap available using the above described sample is 750 nm, between step 525 and 1275 nm. Thus the best intensity cancellation should occur between those two steps.

4. RESULTS

4.1. Tomography

The results of the tomographies are shown in Fig. 5. On the left hand-side the tomographies obtained with the simulated holograms and on the right-hand side those obtained with the experimental holograms. The heights of the two reconstructed sections are those of the bottom (a-0 nm) and the second steps of the sample (b-525 nm). The amplitude images without tomography of the simulated and experimental samples are shown in Fig. 5-(0). The tomographic images show clearly the elimination of the out-of-focus planes. For each plane of interest, the amplitude remains identical as those out of interest get darker as the distance between it and the plane of interest increases. Each step is clearly separated from the others due to the filter produced by the addition of the complex wavefronts. The steps that are separated from the step of interest within a gap smaller than the axial resolution are not clearly eliminated, due to the insufficient attenuation of the filter. The best cancellation is obtained for a gap of 750 nm, as shown in (b) between the plane of interest at 525 nm and the 1275 nm plane. The imperfections in the reconstruction process, like the adjustment of the reference wave parameters and the filtering of the zero order and twin image, influencing both experimental and simulation results, are negligible. Those like the set-up imperfections (lenses, beam-splitters,...) and the wavelengths precision influence only the experimental data. These last variations affect the amplitude of the filter function, but not its zeros. Thus the

attenuation factors can be affected, but not the slicing resolution. Nevertheless, these results show the good cancellation of the planes out of interest and moreover with an attenuation corresponding to the predicted one.

5. CONCLUSION

We have shown that tomography could be achieved at the microscopic scale using Digital Holographic Microscopy (DHM). Simulations and experiments allowed the statement of the method. Slices with a thickness of 725 nm could be achieved, corresponding to the theoretical predictions. This resolution can be improved by taking more holograms in a larger wavelength range. Those results have been achieved using a reflective target to set up the method and the resolution of this new technique. This technique seems promising for 3D bulk specimen investigation.

ACKNOWLEDGMENTS

This study is part of a Ph.D. dissertation performed at the Institute of Applied Optics at the Ecole Polytechnique Fédérale de Lausanne. It was founded through research grants 205320 – 1038 from the Swiss National Science Foundation and supported by Swiss government through CTI grants TopNano 21 #6101.3 and NanoMicro #6606.2 and #7152.1.

REFERENCES

1. L.A. Peach, “Holography finds a home in medicine”, *Laser Focus World* 33 (**12**), pp. 131-135 (1997)
2. E. CuChe, P. Poscio, C. Depeursinge, “Optical tomography at the microscopic scale by means of a numerical low coherence holographic technique”, *Proc. SPIE* **2927**, pp. 61-66 (1996)
3. U. Schnars and W. Jüptner, “Direct recording of holograms by a CCD target and numerical reconstruction”, *Appl. Opt.* 33 (**2**), pp. 179-181 (1994)
4. E. CuChe, F. Bevilacqua, and C. Depeursinge, “Digital holography for quantitative phase contrast imaging”, *Opt. Lett.* 24 (**5**), pp. 291-293 (1999)
5. E. CuChe, P. Marquet, C. Depeursinge, “Simultaneous amplitude-contrast and quantitative phase-contrast microscopy by numerical reconstruction of Fresnel off-axis holograms”, *Appl. Opt.* 38 (**34**), pp. 6994-7001 (1999)
6. D. Carl, B. Kemper, G. Wernicke, and G. von Bally, “Parameter-optimized digital holographic microscope for high-resolution living-cell analysis”, *Appl. Opt.* 43, (**36**), pp. 6536-6544 (2004)
7. P. Marquet, B. Rappaz, and P. J. Magistretti, “Digital holographic microscopy: a noninvasive contrast imaging technique allowing quantitative visualization of living cells with subwavelength axial accuracy”, *Opt. Lett.* 30 (**5**), In press (2005)
8. E. CuChe, P. Poscio and C. Depeursinge, “Optical tomography by means of a numerical low-coherence holographic technique”, *J. Opt.* (**28**), pp. 260-264 (1997)
9. P. Massatsch, F. Charrière, P. Marquet, E. CuChe, C. Depeursinge, “Time domain Optical Coherence Tomography with Digital Holographic Microscopy”, *Appl. Opt.* Accepted for publication
10. E. Wolf, “Three-dimensional structure determination of semi-transparent object from holographic data”, *Opt. Commun.* 1 (**4**), pp. 153-156 (1969)
11. W.H. Carter, “Computational reconstruction of scattering objects from holograms”, *J. Opt. Soc. Am.* 60, (**3**), pp. 306-314 (1970)
12. R. Dändliker, K. Weiss, “Reconstruction of three-dimensional refractive index from scattered waves”, *Opt. Commun.* 1 (**7**), pp. 323-328 (1970)
13. A.F. Fercher, H. Bartelt, E. Becker, H. Wiltchko, “Image formation by inversion of scattered field data: Experiments and computational simulation”, *Appl. Opt.* 18 (**14**), pp. 2427-2439 (1979)
14. J.C. Marron, K.S. Schroeder, “Holographic laser radar”, *Opt. Lett.* 18 (**5**), pp. 385-387 (1993)
15. E. Arons, D. Dilworth, “Analysis of Fourier synthesis holography for imaging through scattering materials”, *Appl. Opt.* 34 (**11**), pp. 1841-1847 (1995)
16. M.K. Kim, “Wavelength scanning digital interference holography for optical section imaging”, *Opt. Lett.* 24 (**23**), pp. 1693-1695 (1999)

17. M.K. Kim, "Tomographic three-dimensional imaging of a biological specimen using wavelength-scanning digital interference holography", *Opt. Express* 7 (**9**), pp. 305-310 (1999)
18. E. Cuhe, P. Marquet, and C. Depeursinge, "Spatial filtering for zero-order and twin-image elimination in digital off-axis holography", *Appl. Opt.* 39 (**23**), pp. 4070-4075 (2000)
19. U. Schnars and W. Jüptner, "Digital recording and numerical reconstruction holograms", *Meas. Sci. Technol* (**13**), pp. R85-R101 (2002)

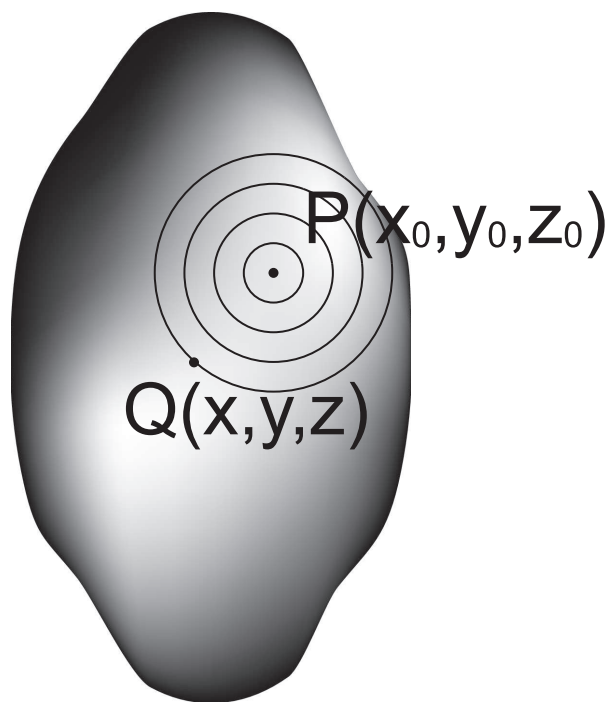


Figure 1. Scheme of the points P and Q in the multi-wavelength approach description

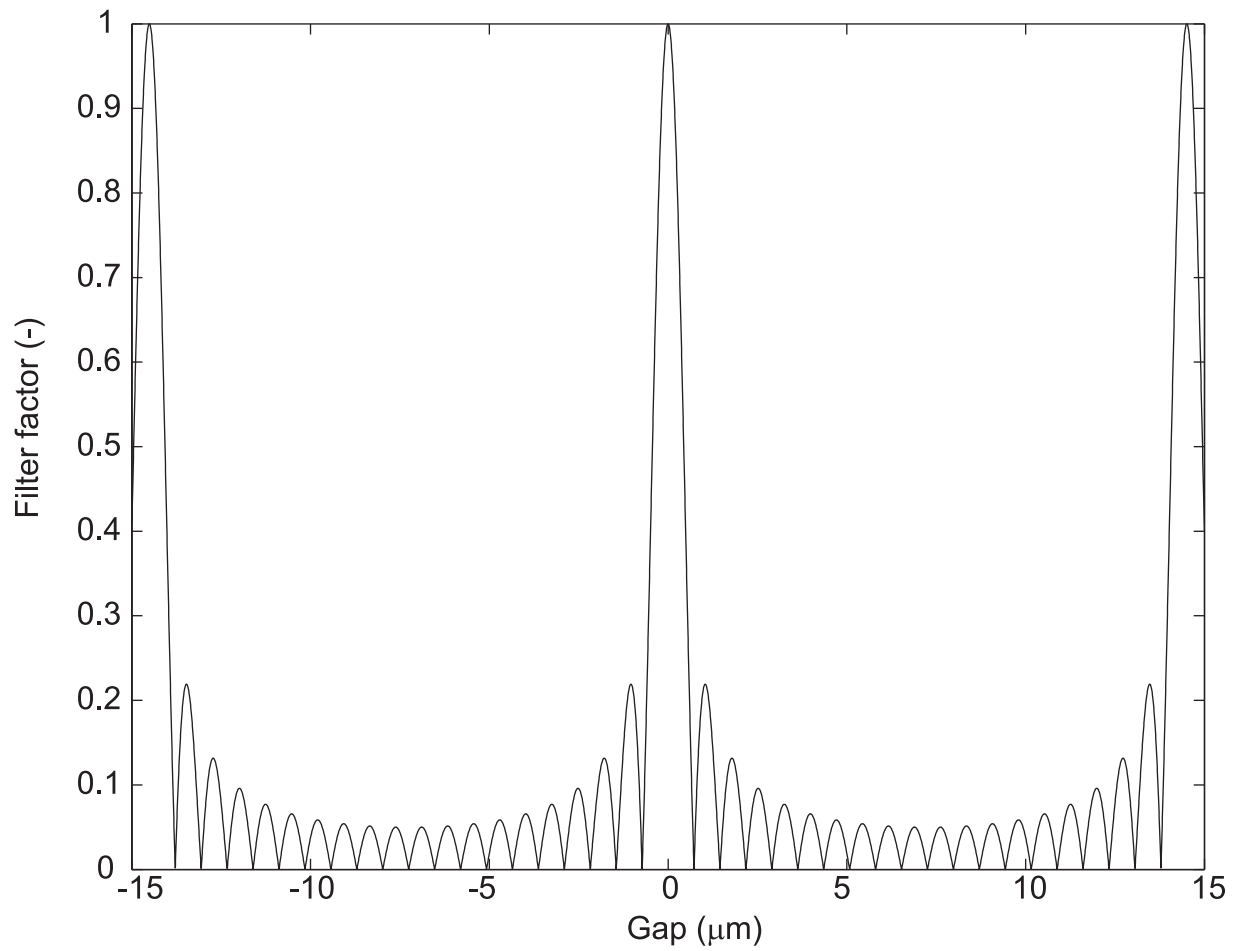


Figure 2. Filter obtained by the sum of 20 k-regularly separated wavelengths taken between 480 and 700 nm. Axial extent $\Lambda=14.5 \mu\text{m}$, axial resolution $\delta=725 \text{ nm}$

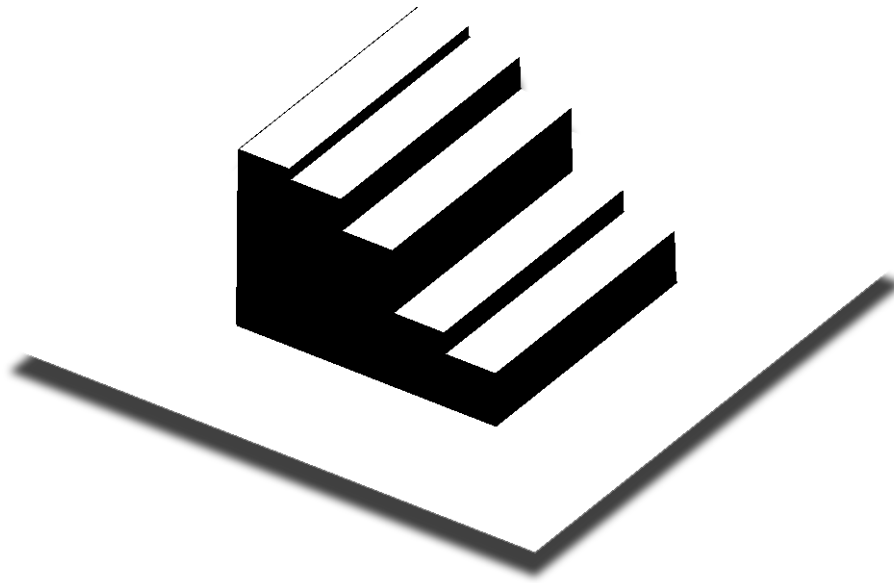


Figure 3. Simulated target with steps of 375, 525, 975, 1200 and 1275 nm

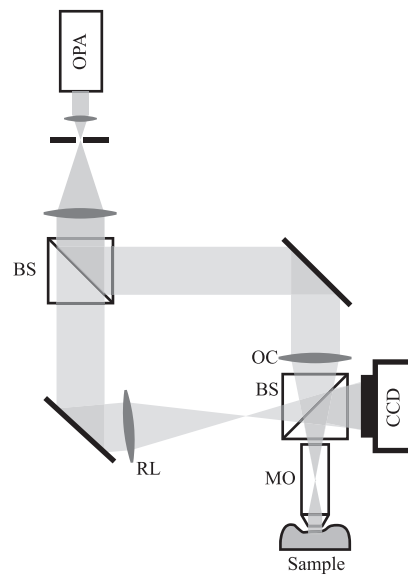


Figure 4. Experimental set-up. OPA: adjustable wavelength laser, BS: beam splitters, MO: Microscope Objective, OC Object Beam Condenser, RL Reference Lens, CCD Charged Coupled Device Camera

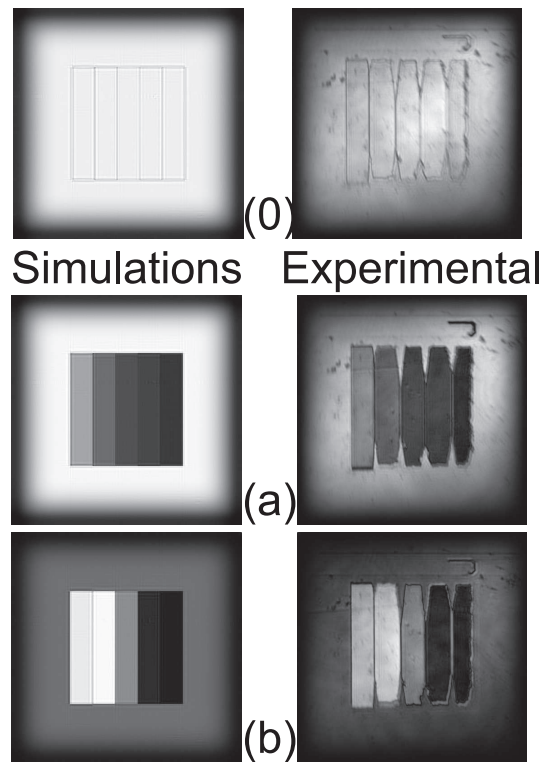


Figure 5. Simulated and experimental results of two reconstructed sections at 0 and 525nm (a, b resp.) as well as the sample amplitudes of the simulated and experimental target (0)